Experimental investigation of evacuated heat pipe solar collector efficiency using phase-change fluid

Wenbo Fang[1*], Saffa Riffat[2] and Yupeng Wu[2]
[1]*School of Architecture and Urban Planning, Shandong Jianzhu University, Jinan 250101, China;* [2]*Department of Architecture and Built Environment, University of Nottingham, Nottingham NG7 2RD, UK*

Abstract

Performance of a microencapsulated phase-change material (PCM) as a heat-transport medium in an evacuated heat pipe solar collector was evaluated and the results compared with those using water. Collector efficiency was experimentally determined according to the method based on European Standard EN 12975–2: 2006. This method proved unsuitable when using an encapsulated PCM suspension. A modified test method was proposed, which was appropriate for predicting solar collector efficiency when using a phase-change fluid. Average solar collection efficiency when using a PCM suspension was higher than that using water.

Keywords: test method EN 12975; phase-change material; encapsulation; solar collector efficiency

*Corresponding author:
wenbo.fang@hotmail.com

Received 17 September 2016; revised 17 June 2017; editorial decision 22 June 2017; accepted 27 June 2017

1 INTRODUCTION

Microencapsulated phase-change material (MPCM) suspensions have been used in thermal systems for energy storage and transportation purposes [1–3]. MPCM suspensions have many advantages over conventional single-phase fluids. The apparent specific heat of a suspension is higher because of its latent heat effect, which can greatly enhance heat-transfer performance between the suspension and heat-transfer surface. Suspensions also have higher thermal energy storage capacity. Furthermore, agglomeration and deposition of particles in the carrier fluid are avoided because the phase-change material (PCM) is separated from the carrier fluid by a thin plastic shell.

Compared with sensible heat storage, application of a PCM as a storage medium is more efficient, because it offers a high thermal energy density in a small temperature differential range, due to its high apparent specific heat during the phase-change process [4]. PCMs are widely used as storage media for air-conditioning, heating, and cooling applications [5]. The major drawback of PCMs is their low thermal conductivity, which affects heat transfer inside the storage tank. Microencapsulation is one technique used to improve these heat-transfer characteristics [6]. Encapsulation methods and their advantages were discussed by Oró *et al.* [7]. It was concluded that microencapsulation is an efficient way to ensure the thermal, structural and chemical stability of PCMs. Existing techniques for microencapsulation were reviewed by Zhai *et al.* [8]. Diaconu *et al.* [9] studied the natural convective heat transfer occurring inside an MPCM. Farid *et al.* [10] compared the mechanical stability of different MPCMs with respect to the number of heating and cooling cycles that could be achieved. Allouche *et al.* [11] studied the thermophysical properties and natural convective heat transfer of an MPCM slurry, comparing the results with those obtained for water.

Studies of MPCM suspension heat-transfer characteristics have been carried out by both theoretical analyses and experimental tests, but most have been based on numerical methodologies. For example, laminar heat-transfer characteristics of an MPCM slurry in a circular tube were investigated numerically [12], where 3D laminar flow and heat-transfer modeling were developed to predict the system performance. A model describing the thermal behavior of PCM slurry flow in a circular duct was developed [3], which could be used to predict the minimal length of the exchanger required for complete freezing of all particles in the slurry. Laminar convective heat-transfer enhancement of an MPCM slurry in a tube with constant heat flux was also investigated numerically and different carrying fluids were

International Journal of Low-Carbon Technologies 2017, 1–8

doi:10.1093/ijlct/ctx010

compared [13]. Most experimental studies reported in the literature were carried out under constant heat flux [14–17] or constant wall temperature [18] conditions.

Studies of the direct application of PCM's as heat transfer fluid (HTF) in solar thermal collectors have been studied extensively in literature and in experiments. For instance, in reference [19], an MPCM slurry thermal energy storage was proposed in a residential solar energy system. Kasza proposed a system that directly uses PCMs inside water based suspensions [20] as an enhanced HTF in the primary loop of solar collector systems. Gianluca *et al.* [21] proposed a flat-plate solar thermal collector with an MPCM slurry, a prototypal system was presented and the possible advantages and drawbacks were discussed. A numerical model was presented and a simulation of a flat-plate solar thermal collector with PCM slurry as HTF were proved by Gianluca *et al.* [22]. Simulations were in fact carried out assuming a fixed and constant flow rate for all the locations and over time.

Differential scanning calorimetry (DSC) is widely used by researchers to determine the phase-change temperature range and quantify the cold storage capacity of PCMs. Scanning method and rate are important factors influencing the accuracy of this results. The stepwise method has been found to be more accurate and less sensitive to operating parameters than the dynamic method [23]. The influence of heating and cooling rates on the precision of DSC results has also been studied: better accuracy is generally obtained at slower scanning rates [24]. Lazaro *et al.* [25] determined the enthalpy of a PCM using three different DSC procedures and identified the influencing factors on the measured results.

The 'European Standard EN 12 975–2: Thermal Solar Systems and Components—Solar Collectors—Part 2: Test Methods' (EN 12 975–2: 2006) is most widely used to evaluated the performance of solar collectors in Europe. For normal fluids, such as anti-freeze and pure water, the standard methods are appropriate; however, for phase-change fluids, such as microencapsulated PCM suspensions, these do not work. Modifications to the test methods are therefore necessary.

In this study, an experimental analysis of the heat transfer in sensible and latent storage mediums using water and an MPCM, under identical operating conditions, was performed. The MPCM slurry was PC210 (Ciba, BASF), used at a concentration of 50% v/v, which has a phase-change temperature around 30°C. This material is assessed for the first time to evaluate its potential to be integrated into a solar thermal energy system.

2 MATERIAL PROPERTIES AND EXPERIMENTAL PROCEDURE

2.1 Characteristics of PCM

The selection of PC210 as the PCM was based on the fact that its phase-change temperature range. The reason of applying PC210 as HTF with a phase change interval between 23 and 32°C is the load application is low temperature heating system such as underfloor heating, its required work temperature is ~30°C. Characterization of the thermal properties of the selected PCM is a key factor for proper understanding of the heat-transfer process in the solar thermal system. The physical properties of PC210, as provided by the manufacturer, are listed in Table 1.

2.2 Morphology of encapsulated PCM

The MPCM was prepared by microencapsulating 99% *n*-octadecane with gelatine using the process of coacervation. The process produces cross-linked microcapsules with diameters in the range of 1–260 μm. Several batches of microencapsulated *n*-octadecane were prepared to determine the best chemical composition (PCM and nucleating agent) to minimize the phenomenon of supercooling and ensure long-term durability of the microcapsules. Figure 1 shows the particle size distribution of the suspension as measured by scanning electron microscopy (SEM).

Table 1. *Physical properties of MPCM suspension (BASF Ciba PC210 Product Instructions).*

Product color	White
Appearance	Emulsion
Mass fraction (%)	46.8
Volume concentration (%)	50
Particle size (μm)	1.62~4.7
Viscosity (cps)	380
DSC calorific value (test method 1597) (J/g)	53
Density of suspension (g/L)	900
Density of capsule (g/L)	800
Thermal conductivity (in the liquid form) (W/m K)	0.4
Specific heat (outside of the phase change region) (J/g K)	3

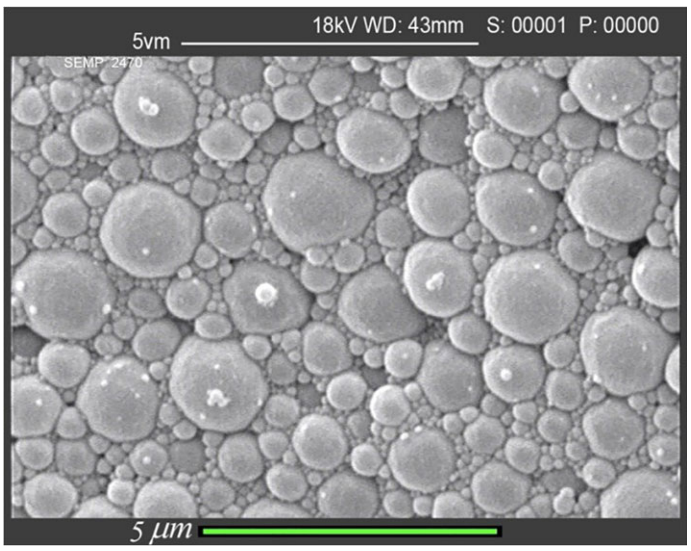

Figure 1. *Encapsulated PC210 as measured by scanning electron microscopy. Mean particle size: 1–2 μm; shell thickness: 100 nm (from Ciba PC210 Manual).*

2.3 Thermal property characterization by DSC

A DSC is often used to determine the thermal properties of micro-encapsulated PCM suspensions, which is a critical step in their characterization. The technique measures the amount of heat absorbed or released by a sample of known mass in comparison with a standard reference heated or cooled at a predefined rate. The resulting energy–temperature curve is used to determine the latent heat of fusion and melting point. More information on DSC methods and equipment can be found in ASTM E 1269. A TA Instruments 2920 Modulated DSC was used to determine the thermal properties of the MPCM suspension. It was calibrated by performing baseline, cell constant and temperature calibration runs. The built-in software compared the data from all the calibration runs and determined the baseline slope, baseline offset, cell constant values and temperature corrections, which were taken into consideration in computing the thermal properties. DSC tests were carried out to measure the latent heat of fusion and melting point of bulk octadecane with and without nucleating agent. the results are shown in Figure 2. The heats of fusion were measured as 47.7 J/g during the heating process and 52.6 J/g during the cooling process, and the melting and crystallization temperatures were determined as 26 and 30.85°C, respectively. The discrepancies were attributed to supercooling. To avoid any degree of supercooling (difference between melting and solidification points), a batch of MPCM containing 0.2% fumed silica as a nucleating agent was prepared.

Figure 3 shows the melting and solidification temperatures as determined by direct experiment: the results are the same as those of the DSC analysis.

The specific heat of the MPCM suspension was calculated according to the formula presented by Hu and Zhang [26] as follows:

$$c_p = c_{p\,.\,b0} \cdot \begin{cases} 1 & (T < T_1) \\ 1 + \dfrac{\pi}{2} \cdot b \cdot \sin\left(\pi \cdot \dfrac{T - T_1}{T_2 - T_1}\right) & (T_1 \le T \le T_2) \\ 1 & (T > T_2) \end{cases}$$

$$b = \frac{c_m \cdot h_{fs}}{c_{p,b0} \cdot (T_2 - T_1)} - \frac{c_m \cdot c_{p,s}}{c_{p,b0}}, \qquad (1)$$

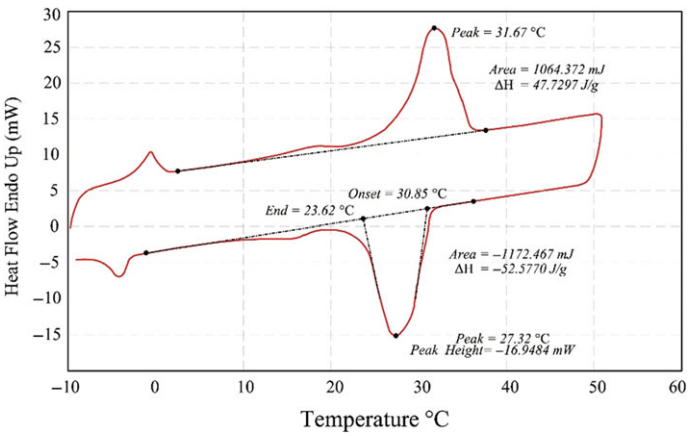

Figure 2. *Differential scanning calorimetry heating and cooling curves for MPCM suspension of PC210.*

where c_p is the specific heat (J kg^{-1} K^{-1}); T is the temperature; b is the bulk fluid (MPCM suspension); s is the shell; and 0 is the non-phase change state.

Figure 4 shows that the Equation (1) can be used to predict the specific heat of PC210 properly.

3 EXPERIMENTAL SYSTEM AND APPROACH

A schematic of the experimental rig is shown in Figure 5. The major components were a suspension reservoir used as the storage tank, a vacuum heat pipe solar collector (consisting of 20 heat pipes and a manifold), a pressure transmitter, a peristaltic pump, an auxiliary heat resource (comprising a boiler with an immersion heater, a cylinder and a coil heat exchanger), a pyranometer, a floodlight array framework and a data acquisition system (computer and DT500 data logger). An environmental chamber was used to simulate different climatic conditions with constant ambient temperature and humidity.

The experiments were carried out in a 100 L horizontal heat storage tank equipped with two coil heat exchangers at the

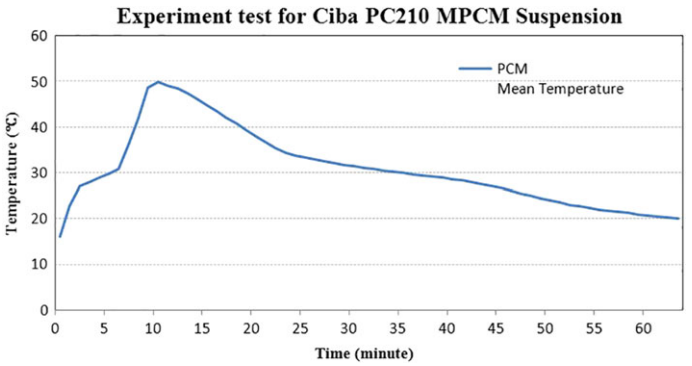

Figure 3. *Experimental determination of thermal parameters of MPCM suspension.*

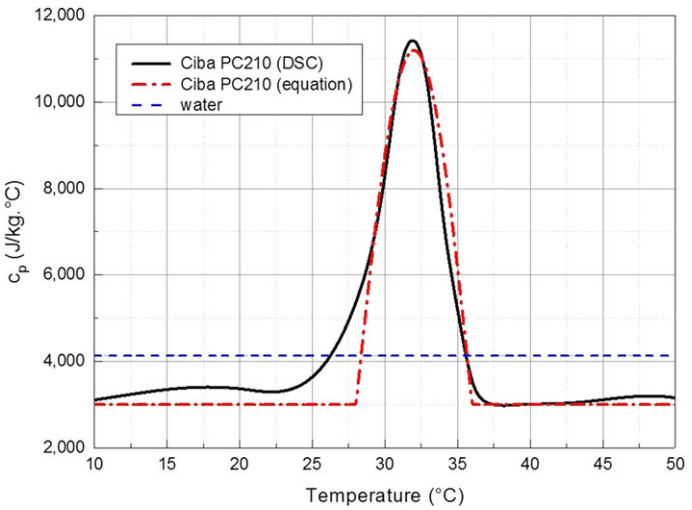

Figure 4. *Specific heat from DSC curve vs that from Equation 1.*

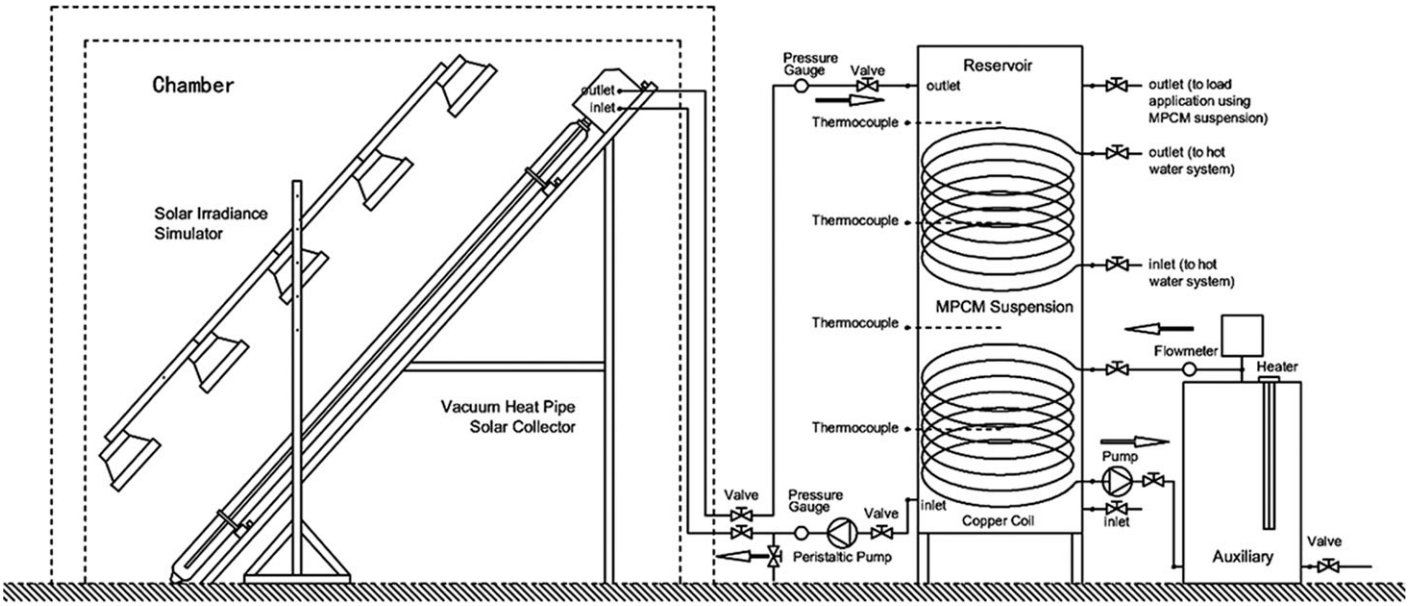

Figure 5. *Schematic of solar thermal energy storage experimental system.*

bottom for the auxiliary charging process, and a similar one at the top to ensure discharging for hot water application. The MPCM slurry was PC210 (Ciba, BASF), used at a concentration of 50% v/v, which has a phase-change temperature around 30°C. This material is assessed for the first time to evaluate its potential to be integrated into a solar thermal energy system.

The solar collector was a Mazdon 20–TMA600s evacuated tube collector, supplied by Thermomax Kingspan Renewables Ltd. (UK). The absorber area of the collector was 2.143 m^2, the gross area was 3.032 m^2, and the aperture area was 2.573 m^2. Its relative efficiency, for a solar irradiance of 800 W/m^2, as supplied by the manufacturer, is shown in Figure 6. The red line shows the solar efficiency based on the absorber area; the blue line shows that based on aperture area, and the green line is based on gross area. In this study, all test results reported are based on the absorber area.

According to the requirements documented in Section 6.1.5.2 of EN 12 975–2: 2006, a floodlight array should be installed as the solar irradiance simulator. In such tests, it is difficult to produce a uniform beam of simulated solar radiation; therefore, it is necessary to measure a mean irradiance level over the collector aperture.

The test procedure accurately followed Section 6.1.5.5 of EN 12 975–2: 2006. Eight test points are considered adequate for testing using solar simulators, provided that at least four different inlet temperatures are used and adequate time is allowed for the temperature to stabilize. One inlet temperature should lie within 3 K of the ambient air temperature.

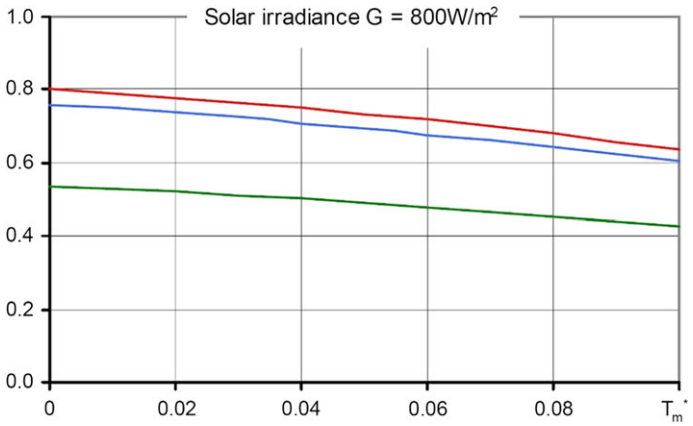

Figure 6. *Solar efficiency of TMA600s (Product Fact Sheet),* $T_m^* = (T_{out} - T_{in})/G$.

4 RESULTS

4.1 Water test

Tests using water as the heat-transport medium were first carried out. The water was passed through the collector manifold at a mass flow rate of 2.4 kg/min. The results obtained (Table 2) were used to calculate the solar collector efficiency (Figure 6) according to the equation prescribed by EN 12 975–2: 2006, where *f* is the single-phase fluid (water) and *A* is the area:

$$\eta = \frac{c_{p,f} \cdot \dot{m} \cdot (T_{out} - T_{in})}{A \cdot G}. \quad (2)$$

From the experimental data shown in Figure 7, it was evident that the solar collector was operating well, according to EN 12 975–2: 2006: the error of efficiency difference between test and fact sheet was <1%, which was within the permissible range.

4.2 Test using MPCM suspension

A test in which the MPCM suspension was employed as the fluid medium was then carried out under the same conditions.

Table 2. *Water test results for TMA600s solar collector (solar irradiance, G = 800 W/m^2; T_a = 20°C, a = ambient; mass flow rate, $\dot{m}$ = 2.4 kg/min).*

T_{in} (°C)	T_{out} (°C)	T_{mean} (°C)	$(T_{mean} - T_a)/G$	$T_{out} - T_{in}$ (°C)	Efficiency (test), η	Efficiency (fact sheet)
21.2	28.4	24.8	0.006	7.20	0.743	0.760
19.8	26.9	23.4	0.004	7.10	0.733	0.753
40.6	47.3	43.9	0.030	6.70	0.691	0.712
41.4	47.9	44.7	0.031	6.50	0.681	0.706
59.4	65.1	62.2	0.053	5.70	0.645	0.671
61.1	66.9	64.0	0.055	5.80	0.642	0.665
79.1	84.2	81.7	0.077	5.10	0.595	0.618
80.3	85.2	82.8	0.078	4.90	0.583	0.609

The experimental data are shown in Table 3. The specific heats, c_p, of the sequences were obtained using Equation (1). The efficiency was calculated from Equation (3) and the results are shown in Table 3 as well:

$$\eta = \frac{c_p \cdot \dot{m} \cdot (T_{out} - T_{in})}{A \cdot G}. \quad (3)$$

Figure 8 shows the results obtained using the traditional test method based on EN 12975–2: 2006. The fitted curve has a significant inflexion. In the phase-change region (Sequences 1 and 2), for Sequence 1, the temperature difference between the inlet and outlet is 8.24°C, and that of the single-phase fluid (water) is 14.2°C; for Sequence 2, they are 7.35 and 12.6°C, respectively. The temperature difference of MPCM slurry is much lower than that of water due to latent heat released during the phase-change process. The qualitative temperature of the specific heat of the heat-transport medium was the mean fluid temperature. If the mean temperature is not within the phase-change region and that of fluid entering the phase-change region during the latter part of the test, the efficiency will be too low, as determined using the traditional test method. EN 12 975–2: 2006 is therefore not suitable for this phase-change fluid.

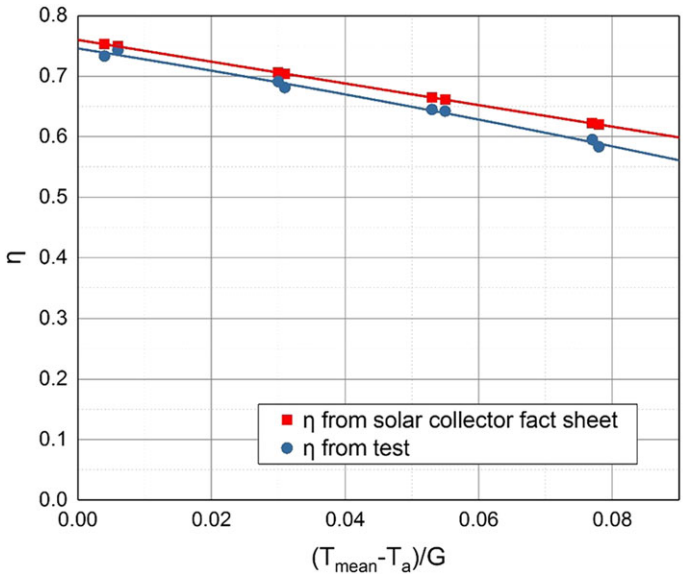

Figure 7. *Relationship between solar collection efficiency, η, and $(T_{mean} - T_a)/G$ as determined from test results for the TMA600s evacuated heat pipe solar collector using water as the heat-transport medium.*

5 MODIFIED SOLAR COLLECTOR EFFICIENCY TEST METHOD

A modified test method for measuring solar collector efficiency was performed, which took into account the phase-change interval of the MPCM suspension. For traditional media, such as water, this approach works very well because the specific heat of water is essentially unchanged during temperature interval, $T_{out} - T_{in}$. This method is suitable for most single-phase fluids that do not undergo a phase change, such as water and glycol.

Owing to phase changes in the MPCM suspension, however, the apparent specific heat is a function of temperature during the phase-change interval and may change immediately when the temperature of the fluid enters this interval. The length of the heat-exchange section with heat pipes in a manifold channel is too short to assume that the specific heat of the suspension remains constant in each section. In the modified test method, the measurement points were selected in the middle of two adjacent heat-exchange sections, so the temperatures before and after the fluid flowed through each heat pipe could be obtained. The measurement points are shown in Figure 9.

As shown in Figure 9, there were $n + 1$ measurement points, including the inlet and outlet temperatures. The results are given in Table 3 and the temperature distributions are presented in Table 4.

The solar collector efficiency was calculated using Equation (4):

$$\eta = \frac{\sum_{i=1}^{n} c_{p,i} \cdot \mathrm{m} \cdot (T_{i+1} - T_i)}{A \cdot G}. \quad (4)$$

The results are shown in Table 5 and Figure 10.

6 COMPARISON BETWEEN EN 12 975–2: 2006 AND MODIFIED METHOD FOR MPCM SUSPENSION

To compare and verify the two test methods for solar collector efficiency, another set of experimental data, in which

Table 3. *Experimental results for solar collector efficiency based on EN 12 975–2: 2006 standard (mass fraction, c_m = 20%, G = 800 W/m^2, flow rate of medium = 2.0 kg/min, T_a = 20°C).*

Sequence number	T_{in} (°C)	T_{out} (°C)	T_{mean} (°C)	$(T_{mean} - T_a)/G$	$T_{out}-T_{in}$ (°C)	Efficiency
1	20.12	28.36	24.24	0.005	8.24	0.580
2	21.51	28.86	25.185	0.006	7.35	0.517
3	42.43	51.2	46.815	0.034	8.77	0.617
4	41.02	50.2	45.61	0.032	9.18	0.646
5	63.67	71.4	67.535	0.059	7.73	0.544
6	60.12	68.76	64.44	0.056	8.64	0.608
7	81.32	88.98	85.15	0.081	7.66	0.539
8	78.89	86	82.445	0.078	7.11	0.501

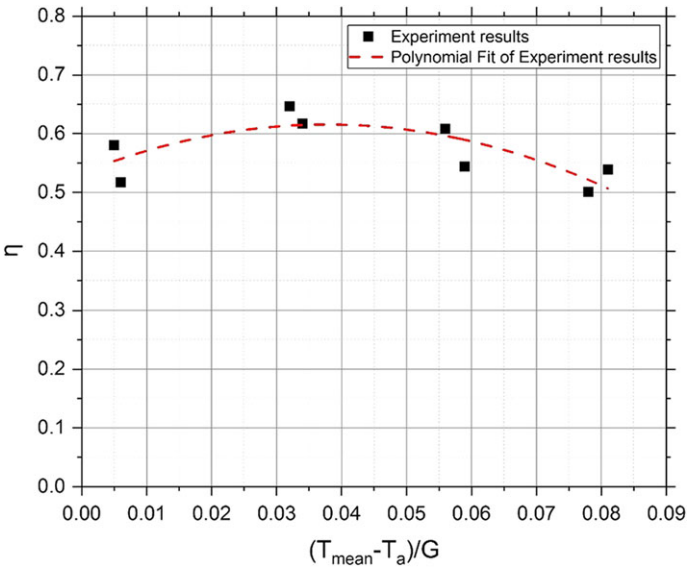

Figure 8. *Solar collector efficiency test results for MPCM suspension, as calculated based on EN 12975–2: 2006 standard.*

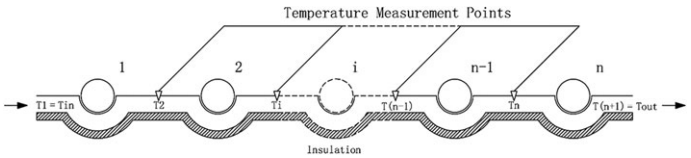

Figure 9. *Location of temperature measurement points for determination of apparent specific heat of an MPCM heat-transfer medium.*

Table 4. *Experimental temperature distributions in test sections for MPCM suspension.*

	Temperature of sequences (°C)							
Measure point	1	2	3	4	5	6	7	8
1	20.12	21.51	42.43	41.02	63.67	60.12	81.32	78.89
2	20.48	21.48	42.46	41.46	63.42	60.44	81.4	78.4
3	20.96	21.96	42.92	41.92	63.84	60.88	81.8	78.8
4	21.44	22.44	43.38	42.38	64.26	61.32	82.2	79.2
5	21.92	22.92	43.84	42.84	64.68	61.76	82.6	79.6
6	22.4	23.4	44.3	43.3	65.1	62.2	83	80
7	22.88	23.88	44.76	43.76	65.52	62.64	83.4	80.4
8	23.36	24.36	45.22	44.22	65.94	63.08	83.8	80.8
9	23.84	24.84	45.68	44.68	66.36	63.52	84.2	81.2
10	24.32	25.32	46.14	45.14	66.78	63.96	84.6	81.6
11	24.8	25.8	46.6	45.6	67.2	64.4	85	82
12	25.28	26.28	47.06	46.06	67.62	64.84	85.4	82.4
13	25.76	26.68	47.52	46.52	68.04	65.28	85.8	82.8
14	26.24	27.04	47.98	46.98	68.46	65.72	86.2	83.2
15	26.66	27.36	48.44	47.44	68.88	66.16	86.6	83.6
16	27	27.64	48.9	47.9	69.3	66.6	87	84
17	27.32	27.9	49.36	48.36	69.72	67.04	87.4	84.4
18	27.6	28.16	49.82	48.82	70.14	67.48	87.8	84.8
19	27.86	28.4	50.28	49.28	70.56	67.92	88.2	85.2
20	28.12	28.64	50.74	49.74	70.98	68.34	88.6	85.6
21	28.36	28.86	51.2	50.2	71.4	68.76	88.98	86

Table 5. *Solar collector efficiency calculation results.*

Sequence number	1	2	3	4	5	6	7	8
Efficiency	0.75	0.758	0.715	0.696	0.655	0.662	0.599	0.608

the PCM concentration was 30% and the mass flow rate was 2.4 kg/min, were selected to calculate the efficiency using the modified test method. The measurement points shown in Figure 9 were employed. The qualitative temperature of the specific heat for each heat-exchange section was given by the mean temperature, $T_{mean,i} = (T_i + T_{i+1})/2$, The results are given in Table 6 and the temperature distribution is shown in Table 7.

According to Equation (1) (a sine curve), and based on the qualitative temperature ($T_{mean,i}$) and the specific heat of each heat-exchange component, the solar collector efficiency was calculated using Equation (4). The results are shown in Table 8.

Figure 11 shows the results of the traditional test method based on EN 12 975–2: 2006 with those of the modified test method for the MPCM suspension. The fitted curve of traditional test method has a significant inflexion. In the phase-change region (Sequences 1 and 2), Table 8 and Figure 11 show the solar collector efficiency in Sequences 1 and 2 are 59 and 56% for the concentration of 30%, and 58 and 51.7% for concentration of 20%, And the efficiency for water are 74.3 and 73.3%. It can be seen that the efficiency of solar collector with MPCM slurry is much lower than that of a single-phase fluid. Figure 11 shows that the modified test worked very well: the

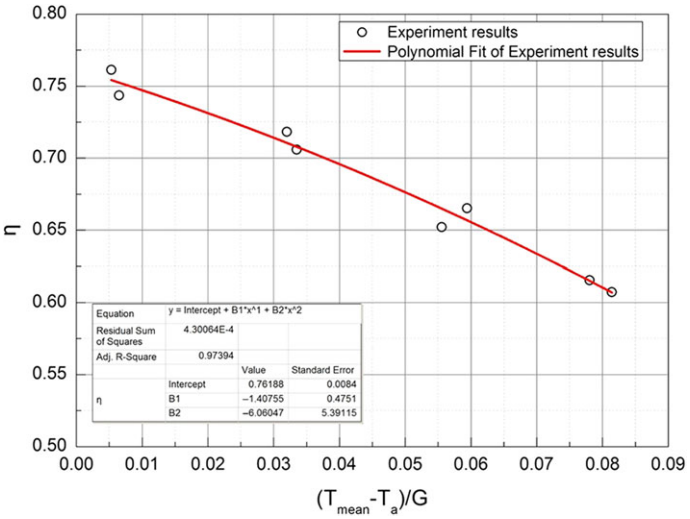

Figure 10. *Experimental results for solar collector efficiency using MPCM suspension as the heat-transfer medium.*

Table 6. *Experimental results for 30% concentration of MPCM slurry.*

Sequence number	T_{in} °C	T_{out} °C	T_{mean} °C	$(T_{mean} - T_a)/G$	$T_{out} - T_{in}$ °C
1	20.11	27.1	23.605	0.005	6.99
2	21.3	28.02	24.66	0.006	6.72
3	40.26	48.47	44.365	0.03	8.21
4	41.11	49.5	45.305	0.032	8.39
5	61.32	68.71	65.015	0.056	7.39
6	62.41	69.54	65.975	0.057	7.13
7	82.63	89.22	85.925	0.082	6.59
8	79.52	86.24	82.88	0.079	6.72

average efficiency when using the MPCM suspension as the heat-transport medium was higher than that using water.

7 CONCLUSIONS

Laboratory tests were carried out to determine the solar collector efficiency using an MPCM suspension as the heat-transport medium. The experimentally determined efficiency was in the range of 60–80% and decreased with increasing value of $(T_{mean} - T_a)/G$. For the MPCM suspension collector, a set of tests were carried out under indoor conditions using a solar simulator.

The results obtained based on the European Standard EN 12 975 test method showed significant inflexion when the heat-transport medium was a MPCM suspension, owing to the phase change of this material. It was necessary to modify the test method for solar collector efficiency when using such suspensions. Comparison of experimental results showed that the modified test method could accurately predict the glazed solar collector efficiency when using the phase-change fluid as the heat-transport medium. The average solar collector efficiency

Table 7. *Results for temperature distribution for MPCM suspension.*

	Temperature of sequences (°C)							
Measure point	1	2	3	4	5	6	7	8
1	20.11	21.3	40.26	41.11	61.32	62.41	82.63	79.52
2	20.64	21.44	40.42	41.42	61.38	62.38	82.36	79.36
3	20.62	21.88	40.84	41.84	61.76	62.76	82.72	79.72
4	21.11	22.32	41.26	42.26	62.14	63.14	83.08	80.08
5	21.74	22.76	41.68	42.68	62.52	63.52	83.44	80.44
6	21.75	23.2	42.1	43.1	62.9	63.9	83.8	80.8
7	21.87	23.64	42.52	43.52	63.28	64.28	84.16	81.16
8	22.57	24.08	42.94	43.94	63.66	64.66	84.52	81.52
9	23.02	24.52	43.36	44.36	64.04	65.04	84.88	81.88
10	23.53	24.96	43.78	44.78	64.42	65.42	85.24	82.24
11	23.26	25.4	44.2	45.2	64.8	65.8	85.6	82.6
12	23.78	25.84	44.62	45.62	65.18	66.18	85.96	82.96
13	24.59	26.28	45.04	46.04	65.56	66.56	86.32	83.32
14	24.70	26.6	45.46	46.46	65.94	66.94	86.68	83.68
15	24.97	26.88	45.88	46.88	66.32	67.32	87.04	84.04
16	25.22	27.12	46.3	47.3	66.7	67.7	87.4	84.4
17	26.00	27.34	46.72	47.72	67.08	68.08	87.76	84.76
18	26.30	27.54	47.14	48.14	67.46	68.46	88.12	85.12
19	26.37	27.72	47.56	48.56	67.84	68.84	88.48	85.48
20	27.10	27.9	47.98	48.98	68.22	69.22	88.84	85.84
21	27.10	28.02	48.47	49.50	68.71	69.54	89.22	86.24

Table 8. *Efficiency calculation results for MPCM suspension.*

Sequence number	1	2	3	4	5	6	7	8
η(water)	0.743	0.733	0.691	0.681	0.645	0.642	0.595	0.583
η(30%, EN 12975)	0.59	0.568	0.694	0.679	0.624	0.602	0.557	0.568
η(30%, Modified)	0.771	0.764	0.716	0.728	0.675	0.662	0.617	0.61
η(20%, EN 12975)	0.58	0.517	0.617	0.646	0.544	0.608	0.539	0.501
η(20%, Modified)	0.75	0.758	0.715	0.696	0.655	0.662	0.599	0.608

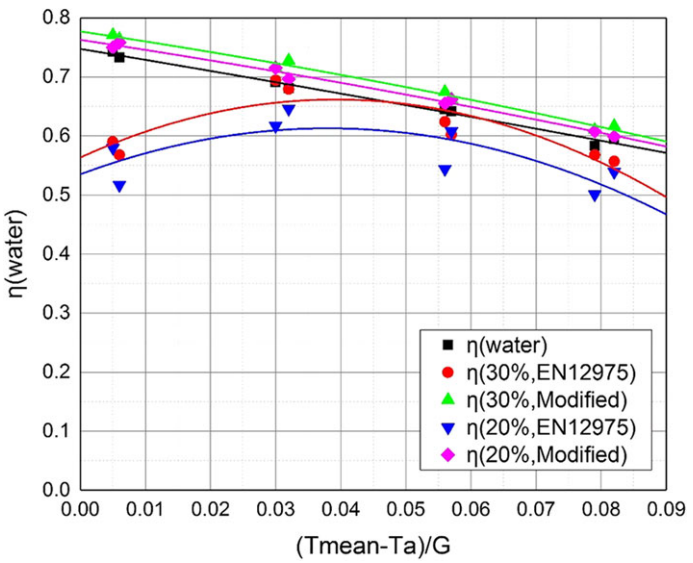

Figure 11. *Comparison between EN 12 975–2: 2006 and modified test method for MPCM suspension.*

when using the MPCM suspension as the heat-transport medium was higher than that using water. At temperatures below 4°C, the MPCM suspension collector average efficiency was ~76%, while that of the traditional solar collector was ~72%; however, because operating temperatures of solar collectors are typically much higher than 40°C, this benefit has little practical relevance.

To validate the accuracy of the modified test method and investigate the performance of other MPCM suspensions, further experiments should be carried to include testing of the MPCM in different types of solar collectors (at low and high temperatures) and the use of other MPCMs with different phase-change temperature ranges. Full-scale demonstration of the technology in actual buildings is also required.

ACKNOWLEDGEMENTS

This work was carried out at the Department of Architecture and Built Environment, University of Nottingham. Funding from the National Natural Science Foundation of China (Grant no. 51 408 340), the Science and Technology Project of Housing and Urban–Rural Construction of Shandong China, 2016 (Title: Research on Design Method of Green Building Skin Integrated with Heat Storage Based on Solar Energy and Latent Heat Utilization Technology), the Science and Technology Project of Housing and Urban–Rural Construction of Shandong China, 2017 (Grant no. 2017-K3-005), the Science and Technology Program of Jinan China (Grant no. 201 409 043), the Foundation of Shandong Co-Innovation Center of Green Building (Title: Research on Performance of a Novel Solar Hot Water System with Phase Change Energy Storage), and the Foundation of China Scholarship Council (Grant no. 201 409 995 005) is acknowledged.

REFERENCES

[1] Diaconu BM, Varga S, Oliveira AC. Experimental assessment of heat storage properties and heat transfer characteristics of a phase change material slurry for air conditioning applications. *Appl Energy* 2010;**87**:620–8.

[2] San A, Alkan C, Karaipekli A, *et al.* Microencapsulated n-octacosane as phase change material for thermal energy storage. *Sol Energy* 2009;**83**:1757–63.

[3] Zhang S, Niu J. Experimental investigation of effects of supercooling on microencapsulated phase-change material (MPCM) slurry thermal storage capacities. *Sol Energy Mater Sol Cell* 2010;**94**:1038–48.

[4] Silakhori M, Metselaar HSC, Mahlia TMI, *et al.* Palmitic acid/polypyrrole composites as form-stable phase change materials for thermal energy storage. *Energy Convers Manage* 2014;**80**:491–7.

[5] Rastogi M, Chauhan A, Vaish R, *et al.* Selection and performance assessment of Phase Change Materials for heating, ventilation and air-conditioning applications. *Energy Convers Manage* 2015;**89**:260–9.

[6] Zhang Y, Rao Z, Wang S, *et al.* Experimental evaluation on natural convection heat transfer of microencapsulated phase change materials slurry in a rectangular heat storage tank. *Energy Convers Manage* 2012;**59**:33–9.

[7] Oró E, de Gracia A, Castell A, *et al.* Review on phase change materials (PCMs) for cold thermal energy storage applications. *Appl Energy* 2012;**99**: 513–33.

[8] Zhai XQ, Wang XL, Wang T, *et al.* A review on phase change cold storage in air-conditioning system: materials and applications. *Renew Sust Energy Rev* 2013;**22**:108–20.

[9] Diaconu BM, Varga S, Oliveira AC. Experimental study of natural convection heat transfer in a microencapsulated phase change material slurry. *Energy* 2010;**35**:2688–93.

[10] Farid MM, Khudhair AM, Razack SAK, *et al.* A review on phase change energy storage: materials and applications. *Energy Convers Manage* 2004; **45**:1597–615.

[11] Allouche Y, Varga S, Bouden C, *et al.* Experimental determination of the heat transfer and cold storage characteristics of a microencapsulated phase change material in a horizontal tank[J]. *Energy Convers Manage* 2015;**94**:275–85.

[12] Song S, Liao Q, Shen W. Laminar heat transfer and friction characteristics of microencapsulated phase change material slurry in a circular tube with twisted tape inserts. *Appl Therm Eng* 2013;**50**:791–8.

[13] Song S, Liao Q, Shen W, *et al.* Numerical study on laminar convective heat transfer enhancement of microencapsulated phase change material slurry using liquid metal with low melting point as carrying fluid. *Int J Heat Mass Trans* 2013;**62**:286–94.

[14] Zeng R, Wang X, Chen B, *et al.* Heat transfer characteristics of microencapsulated phase change material slurry in laminar flow under constant heat flux. *Appl Energy* 2009;**86**:2661–70.

[15] Chen B, Wang X, Zeng R, *et al.* An experimental study of convective heat transfer with microencapsulated phase change material suspension: Laminar flow in a circular tube under constant heat flux. *Exp Therm Fluid Sci* 2008;**32**:1638–46.

[16] Alvarado JL, Marsh C, Sohn C, *et al.* performance of microencapsulated phase change material slurry in turbulent flow under constant heat flux. *Int J Heat Mass Trans* 2007;**50**:1938–52.

[17] Royon L, Guiffant G. Forced convection heat transfer with slurry of phase change material in circular ducts: a phenomenological approach. *Int J Heat Mass Trans* 2011;**54**:5554–67.

[18] Zhang Y, Wang S, Rao Z, *et al.* Experiment on heat storage characteristic of microencapsulated phase change material slurry. *Sol Energy Mater Sol Cell* 2011;**95**:2726–33.

[19] Huang MJ, Eames PC, McCormack S, *et al.* Microencapsulated phase change slurries for thermal energy storage in a residential solar energy system. *Renew Energy* 2011;**36**:2932–9.

[20] Kasza KE, Chen MM. Improvement of the performance of solar energy or waste heat utilization systems by using phase-change slurry as an enhanced heat-transfer storage fluid. *J Sol Energy Eng* 1985;**107**:229–36.

[21] Serale G, Fabrizio E, Perino M. Design of a low-temperature solar heating system based on a slurry Phase Change Material (PCS). *Energy Build* 2015; **106**:44–58.

[22] Serale G, Goia F, Perino M. Numerical model and simulation of a solar thermal collector with slurry Phase Change Material (PCM) as the heat transfer fluid. *Sol Energy* 2016;**134**:429–44.

[23] Günther E, Hiebler S, Mehling H, *et al.* Enthalpy of phase change materials as a function of temperature: required accuracy and suitable measurement methods. *Int J Thermophys* 2009;**30**:1257–69.

[24] Castellón C, Günther E, Mehling H, *et al.* Determination of the enthalpy of PCM as a function of temperature using a heat-flux DSC—a study of different measurement procedures and their accuracy. *Int J Energy Res* 2008;**32**:1258–65.

[25] Lazaro A, Peñalosa C, Solé A, *et al.* Intercomparative tests on phase change materials characterisation with differential scanning calorimeter. *Appl Energy* 2013;**109**:415–20.

[26] Hu X, Zhang Y. Novel insight and numerical analysis of convective heat transfer enhancement with microencapsulated phase change material slurries: laminar flow in a circular tube with constant heat flux[J]. *Int J Heat Mass Trans* 2002;**45**:3163–72.